E-ISSN 2586-9027
Homepage : https://tci-thaijo.org/index.php/SciTechAsia Science & Technology Asia
Vol.31 No.1 January - March 2026 Page: [112-124]
Original research article

Investigation on Build Orientation for High Quality and High Tensile Strength Additive Manufacturing Parts

Sunil Kumar Tiwari[1], Yashwant Kumar Modi[2,*], Sarang Pande[3], Vivek Kumar Barnwal[4]

[1]*Department of Mechanical Engineering, O.P. Jindal University, Raighrh 496001, India*
[2]*Department of Mechanical Engineering, Jaypee University of Engineering and Technology, Madhya Pradesh 473226, India*
[3]*Department of Mechanical Engineering, Sir Visvesvaraya Institute of Technology, Nashik 422502, India*
[4]*Department of Manufacturing Engineering, School of Mechanical Engineering, Vellore Institute of Technology, Vellore 632014, India*

Received 30 April 2025; Received in revised form 12 December 2025
Accepted 16 January 2026; Available online 27 March 2026

ABSTRACT

Polyamide-12 (PA 2200) from EOS GmbH is widely used in selective laser sintering (SLS) processes, but its powder quality degrades with repeated use, leading to powder loss. To maintain part quality, 50 to 70 percent of the used powder is regenerated, with only 8 to 12 percent of fresh powder contributing to usable parts. Aged powder must be removed to ensure desired mechanical properties. This study examines how build orientation affects the tensile properties and surface quality of parts made with EOSINT P395 and PA2200 powder, using Taguchi's design of experiments. Results show that specimens printed in the z-axis orientation had the lowest tensile strength, while those in the x-axis orientation exhibited the highest values (43.47 MPa to 46.15 MPa). Additionally, combining new and aged powder, along with post-heating treatment, improved the surface quality of parts, particularly when reclaimed powders were reused.

Keywords: Build orientation; PA2200; Selective laser sintering; Tensile properties; Surface quality

***Corresponding author:** yashwant.modi@juet.ac.in **doi:** xx.xxxxx/scitechasia.xxxx.xx

1. Introduction

The SLS process is a powder bed fusion-based additive manufacturing (AM) technique that utilizes a CO_2laser as a heat source. It employs materials in powder form, selectively heating and fusing the powder particles to form complete layers [1]. Thermoplastics, particularly polyamides such as PA12 (Nylon 12), are commonly used as the primary engineering materials in SLS due to their ability to be processed through partial melting, resulting in parts with improved mechanical properties [2]. The SLS process typically uses thermoplastics, with semi-crystalline materials like polyamide (PA12 or Nylon 12) being the most common powder materials for fabrication [3, 4]. However, other thermoplastics, metallic powders, and composites are also utilized in SLS to produce parts for various applications [5-10]. 3D Systems and EOS are major suppliers of commercially available PA12 powders. These companies market materials such as DuraForm and PA2200, which are widely used for additive manufacturing (AM) of functional parts [11, 12].

The heating process in various AM systems varies depending on the technology and materials used. The EOSINT P395, an EOS SLS machine, features a radiant heater located at the top of the system in the process chamber, and two convector heaters positioned at an angle on the sides of the removal build frame (removal chamber). The heating of powder and maintaining a temperature gradient is a critical aspect of the SLS process, as widely reported by Alimardani [13]. This effect has been extensively studied by Gibson and Shi [14], who observed that if the temperature difference between the process and removal chambers is too large, it may lead to warping and delamination within the layers of the part. Warping in plastic parts is commonly caused by improper cooling, as plastics are poor conductors of heat [15]. They act as insulating media, preventing efficient heat transfer from the inner core to the outer surfaces. As a result, the outer surfaces solidify before the inner core, as noted by Tiwari et al. [1]. Moreover, the outer surface cools and contracts earlier, pulling the soft inner core outward. This deformation, known as warpage, has been widely reported in the literature [1-3, 16, 17]. Parts with larger flat areas are more prone to warping than those with smaller flat surfaces. The effect of warpage can be minimized in the SLS process by increasing the height of the part, as suggested by [2, 3, 12]. However, since AM parts are built layer by layer, the effective height increases with each successive layer, which contributes to warping. If warping is excessive, it can cause delamination of the layers. Additionally, it has been widely studied and reported [1-3, 18] that delamination may also occur if the previously laid layer fails to adhere or fuse with the current layer.

To ensure proper powder spreading during the sintering process and to achieve optimal bonding between powder grains, a typical melt flow rate or viscosity must be maintained. Virgin powder, which has a lower melt flow rate, cannot be used alone; it must be mixed with recycled powder to achieve the required viscosity. The recycled powder is sieved and allowed to settle in a dry atmosphere to eliminate any static charge before mixing. This process is known as powder regeneration for the SLS process and is useful for improving the surface quality and reducing the cost. For quality SLS parts, it is recommended to regenerate powder with 50 to 70 percent of used powder [19-25]. However, excessive recycling without adding sufficient new mate-

rial can degrade part quality, resulting in uneven texture and poor surface finishing. This phenomenon, known as "orange peel," occurs because the surface of the part resembles the skin of an orange [1-3].

In the SLS process, the powder material is pre-heated, and a CO_2 laser, controlled by a scanning system, traces each slice of the model. This process selectively applies heat to fuse the powder particles together, forming a solid part with the desired shape. Prolonged exposure of the powder to heat in the part build chamber can degrade the material properties, as the powder is subjected to temperatures of around 150°C for 10 to 12 hours during a single run. Lowering the temperature in the removal chamber can help reduce the ageing effects on the powder, although this increases the heating time, cycle time, and the risk of warping and delamination [26, 27].

This study is focused on evaluating how the build orientation and powder regeneration collectively influence tensile strength, anisotropy and surface quality in SLS-manufactured parts. The findings provide improved process guidelines and demonstrate measurable reductions in surface defects and dimensional inaccuracies compared to established approaches supporting more consistent SLS manufacturing.

2. SLS Process Parameters

The mechanical properties and appearance quality of SLS-processed parts depend on several factors, including powder material properties, part processing parameters, the binding mechanism, part orientation, and post-processing. The factors affecting the quality of sintered parts can be broadly classified into two categories: (i) factors related to the process, and (ii) factors related to the material properties, as reported by Tiwari et al. [1].

2.1 Factors linked with the process

To achieve the best surface appearance, surface texture, mechanical properties, and part build rate, the part-building process parameters, specifically layer thickness, hatch distance, scan speed of the laser, laser power, powder bed temperature, laser beam spot size, and the chosen scanning pattern must be optimized under conditions designed for each factor [28-40]. For repeatable results, maintaining a uniform and steady powder bed temperature is essential [1, 20]. The selection of different process parameters and their potential effects include: i) Low part bed temperature and low laser power: This combination results in improved dimensional accuracy but lowers part density and increases the likelihood of layer delamination, ii) High laser power and low part bed temperature: This combination increases the tendency for non-uniform shrinkage and the development of residual stresses, which may cause part curling, iii) High part bed temperature and high laser power: This leads to denser parts, but can also result in part growth, iv) Large sintering depth and melt pool diameter: These are achieved by increasing the laser's dwell time in a specific location and using low laser power, which facilitates correct particle fusion at low scan speeds, v) Shorter scan vectors: These lead to more uniform temperature distribution during sintering, as it takes less time to scan the next part, minimizing heat loss vi) High energy density: This results in higher part density and tensile strength, although increasing laser power beyond a certain point may limit further improvements [1, 20, 15].

The mechanical properties of the part are generally improved at the center of the build height compared to extreme positions

[9, 12]. A flat sectional sintering geometry is attainable at higher beam scanning speeds [1, 25]. Increasing laser dwell time improves sintering depth, while the packing density of fabricated parts is enhanced with a combination of higher laser power and lower scanning speed. Additionally, increasing laser power improves both sintering width and depth. High-density parts can be achieved using a zig-zag scanning pattern, as reported by Kumar [41]. Moreover, controlled microstructure and optimal process parameters enhance part characteristics, thereby improving part quality. Optimizing process parameters also leads to better performance and efficiency of the SLS machine. Understanding computational modeling and applying it to optimize varying process parameters can further enhance performance [21]. Gibson and Shi [25] described the relationship between material properties and SLS fabrication parameters, as discussed below.

The relationship for polymer material based on SLS fabrication parameter and material properties are stated as

$$P = \frac{BS \cdot \rho \cdot D_b \cdot h \cdot [C \cdot (T_m - T_B) + l_f]}{(1 - R)}, \tag{2.1}$$

where, T_g is glass transition temperature and T_m is melting temperature of the polymer, part bed temperature (T_b) determines by T_g and T_m temperatures, scan speed (SS), P is fill laser power, and scan spacing (SCSP). In addition, ρ is powder density, C is specific heat, R is reflectivity, l_f is latent melting heat and Db is the diameter of the laser beam on the part bed. f in the following formula represents conversion factor.

$$Energr\ density\left(\frac{cal}{cm^2}\right) = \frac{P \cdot f}{(BS \cdot SCSP)}. \tag{2.2}$$

2.2 Factors linked with the material properties

The density of parts fabricated via SLS can be enhanced by using a blend of powders with different particle sizes. Finer particles, which have a larger surface area, absorb more laser energy, resulting in an increase in operational temperature and, consequently, improved sintering kinetics [15]. The initial packing density significantly influences the final density of the SLS part. Additionally, the rigid network of high-melting-point solid particles in high-sintering-density regions hinders the flow and rearrangement of low-melting-point particles. Conversely, in regions with lower sintering density, the liquid phase can flow more freely, aiding in the rearrangement of solid particles and promoting densification. Material viscosity also impacts the density of SLS-fabricated parts, with higher viscosity typically leading to higher part density. The quality of the part varies during the melting process, with factors such as shrinkage and precision being influenced by the material's crystalline characteristics. Greater deviations between the melting peak and crystalline peak correlate with higher dimensional precision. The minimum layer thickness in SLS is determined by the powder particle size, which directly affects the accuracy of the fabricated part. Smaller particle sizes are preferred for better precision. However, these smaller particles are more prone to oxidation due to their larger surface area compared to larger particles [42-49].

3. Material and Method

Prior to processing parts on the SLS machine, it is essential to select the appropriate SLS material and determine the machine process parameters. For this investigation, polyamide (PA12), developed

by EOS GmbH and marketed as PA2200, is chosen as the SLS material due to its popularity in additive manufacturing (AM) of functional parts. Known for its high strength, durability, and excellent flexibility, PA2200 is ideal for producing functional prototypes, end-use parts, and complex geometries. This powder offers good resistance to abrasion, chemicals, and temperature variations, making it versatile for a wide range of industries, including automotive, aerospace, and healthcare.

The test specimen for this study was prepared according to the ASTM D638-10 standard [50], following the recommendations of the F42 committee's reports ASTM 52921 [51] in Solidworks, a CAD modeling software. The CAD model was saved into .stl file format. Then it was loaded in MagicsRP software to fix errors and prepare build volume. The orientations of the test specimens relative to the coordinate axes were selected according to L9 orthogonal array by Taguchi's design of experiments approach. The sequence of orientations was determined and fixed as follows: first around the x-axis, then the y-axis, and finally the z-axis. The minimum angle was set at 0°, and the maximum angle at 90°, with larger angles corresponding to symmetric conditions within the 0° to 90° range. The nine orientations according to L_9 array are shown in Table 1. Five specimens per orientation were placed in the build preparation as shown in Fig. 1.

To achieve superior quality parts, the optimal values for the process parameters must be carefully selected and set. The key SLS machine operating conditions are outlined according to the EOS GmbH standard operating manual for the EOSINT P395 SLS machine [50], as follows: i) Nominal CO_2 Laser power: 50 W; ii) Wavelength (λ): 10.2 to 10.8 μm; iii) Heater power: removal chamber: 2 kW, process chamber: 2.4 kW; iv) Temperature: removal chamber: 150 °C, process chamber: 176 °C; v) Layer thickness: 0.12 mm. The printer was allowed to warm for 2 h before the desired temperature reached inside the build chamber. For proper investigation, five specimens were prepared for each orientation in the experimental setup All the 45 specimens were printed, removed and cleaned thoroughly after cooling of the build chamber. Fig. 2 shows a photograph of the fabricated specimens. Furthermore, the laser-sintered specimens were tested using a tensile testing machine, Instron 3369, as shown in Fig. 3.

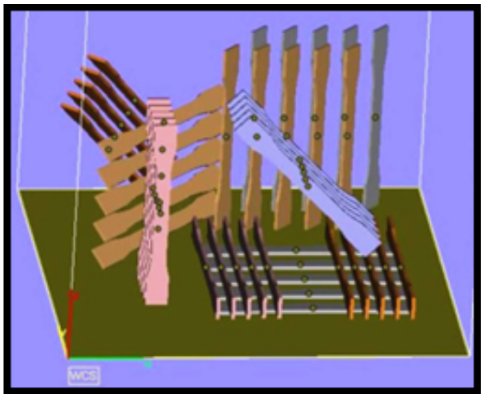

Fig. 1. Build preparation of CAD models in MagicsRP software.

4. Results and Discussion

4.1 Part build orientation

The variations in tensile properties with build orientation shown in Table 1 are as follows:

The average ultimate stress experienced by the specimen ranges from 43.47 MPa to 46.15 MPa. The anisotropic nature of the PA12 material in CO2 laser sintering has been documented by early users of SLS technology. To enable part fabrication in any orientation, it is desirable to mini-

Table 1. Tensile stress and strain of specimens with different orientations.

Part Orientation Around	Specimen No.	Max Stress (MPa)	Average Max Stress (MPa)	Std Dev Max Stress (MPa)	Max Strain at break point	Average Max Strain	Std Dev Max Strain
0	1	46.68	46.15	0.69	39.18	32.77	4.54
0	2	46.40			33.01		
0	3	45.10			32.29		
	4	45.62			34.30		
	5	46.95			25.08		
0	1	44.16	44.60	0.32	27.81	29.46	2.10
45	2	45.06			30.77		
45	3	44.72			30.13		
	4	44.73			32.21		
	5	44.33			26.36		
0	1	45.07	44.90	0.37	31.09	31.59	3.42
90	2	44.82			26.60		
90	3	44.38			36.62		
	4	45.50			29.81		
	5	44.73			33.82		
45	1	44.92	45.76	0.56	31.25	36.16	3.52
0	2	45.80			34.06		
45	3	45.89			36.46		
	4	45.54			37.18		
	5	46.65			41.83		
45	1	44.33	43.84	0.43	30.93	33.30	1.90
45	2	43.34			34.94		
90	3	44.38			36.06		
	4	43.58			32.53		
	5	43.57			32.05		
45	1	44.43	43.47	0.84	24.76	27.08	2.24
90	2	42.31			25.16		
0	3	43.49			30.13		
	4	42.78			25.96		
	5	44.34			29.41		
90	1	46.57	46.10		31.25	32.26	1.80
0	2	44.87			32.61		
90	3	46.51		0.62	34.62		
	4	46.28			29.41		
	5	46.26			33.42		
90	1	44.92	44.47	0.55	31.09	29.68	0.87
45	2	44.85			30.13		
0	3	43.86			29.17		
	4	43.73			29.49		
	5	44.98			28.53		
90	1	43.96	43.93	0.40	21.72	25.85	3.65
90	2	44.42			26.44		
45	3	43.78			21.64		
	4	44.25			30.53		
	5	43.27			28.93		

mize anisotropy without compromising the mechanical properties of the parts. This anisotropy can be explained by the layer-by-layer additive process of the powder bed fusion SLS technique.

Initially, the powder is heated to a temperature just below the melting point of the PA2200 material. As the laser scans across the powder bed along a single vector, the heat from the laser is sufficient to melt the powder. Adjacent molten grains fuse together, forming necks between them,

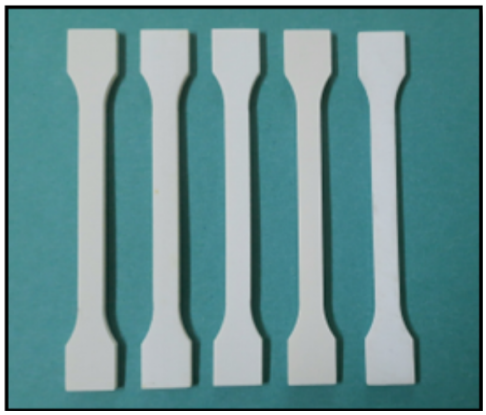

Fig. 2. Photograph of the specimens fabricated along 0 0 0 orientations.

Fig. 3. Experimental set-up for tensile testing.

as shown in Fig. 4(a). When the laser scans the next parallel vector, the level of necking between particles in this new vector will be similar to that in the first vector (Fig. 4(b)). However, the necking between particles across the two vectors will be reduced, as the particles from the previous vector have cooled slightly in preparation for the next scan. The bonding between particles in different layers will be further diminished (Fig. 4(c)) due to the deposition of a new layer of powder over the previously sintered layer [21]. As a result, weaker properties are observed when stress is applied perpendicular to this layer-to-layer bonding.

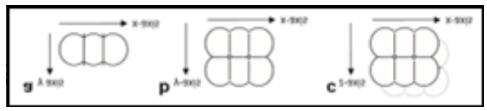

Fig. 4. Schematic delineation of sintering amid the laser sintered process, with (a) demonstrating necking between particles in a solitary vector, (b) necking between two parallel vectors, and (c) necking between various layers.

The parts produced in the z-axis orientation exhibited the lowest tensile strength (see Table 1), while those produced in the x-axis orientation displayed the highest tensile strength. Therefore, based on the manufacturer's recommendations, it is advisable to orient the part so that the largest dimensions lie in the X-Y plane, with the height being the smallest dimension of the part. The main effects of orientation for means, as determined by Taguchi's design of experiments – L_9 array for 3 input parameters (angles of orientation with x-axis, y-axis and z-axis) with 3 levels (0°, 45°, and 90°), are plotted in Fig. 5, while the main effects considering the signal-to-noise (S/N) ratio, using the "larger-the-better" criterion indicating the output desired tensile stress set to be maximum, are shown in Fig. 6. According to S/N ratio, best tensile strength is obtained on 0 0 90 orientation, i.e. the part should be oriented at 0° around x-axis, 0° around y-axis and 90° around z-axis. Figs. 7-9 display the contour plots for the predicted values of tensile stress based on different orientations. In these plots, the green regions indicate pre-

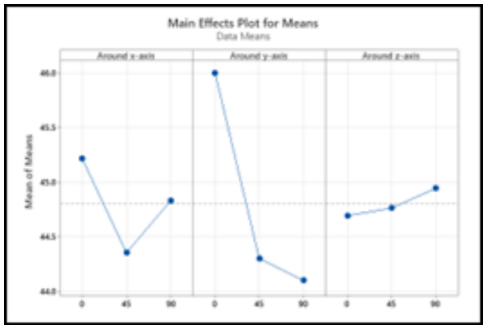

Fig. 5. Main Effect Plot for Means.

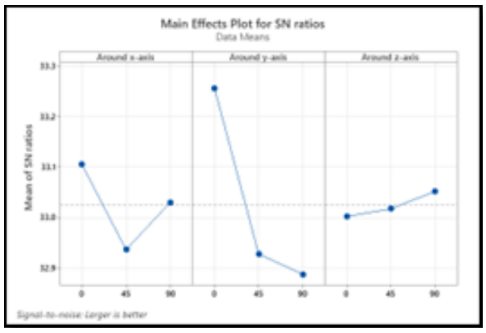

Fig. 6. Main Effect Plot for S/N Ratios.

ferred build orientation angles with respect to different axes, the lower values of standard deviation indicated in the table 1 also synchronize with the green area while the higher values coincide with the blue area in the figures, indicating that if parts are manufactured keeping the orientations in green region, uniform properties will be achieved in manufactured part as they are associated with better predicted tensile properties compared to the blue regions.

4.2 High surface quality

The quality of parts varies with process parameters, binding mechanisms, post-processing, and the use of different combinations of virgin and recycled powders. To maintain the required melt flow viscosity and surface quality, the used powder is mixed with virgin powder after each cycle to achieve high-strength parts with improved surface quality. The experimental results reveal the following: i) Parts made with 100% new powder and varying post-heating times exhibit similar surface properties, indicating that post-heating has little effect on the surface quality of parts made with 100% virgin powder, ii)

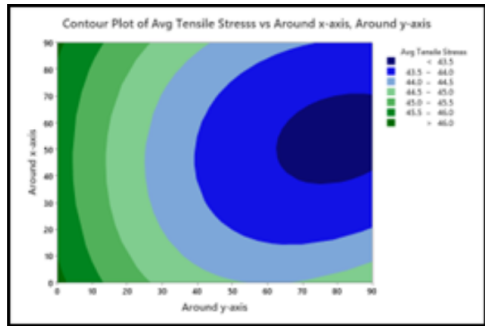

Fig. 7. Contour Plot for tensile stress with respect to X-Y orientation.

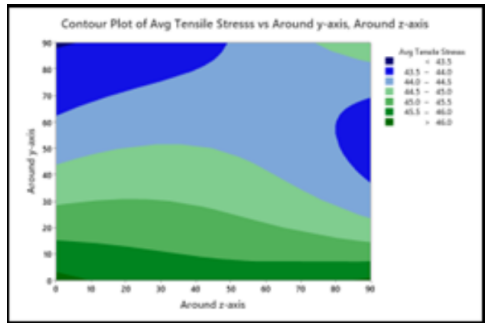

Fig. 8. Contour Plot for tensile stress with respect to Y-Z orientation.

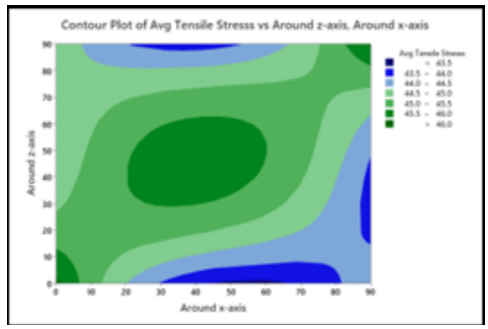

Fig. 9. Contour Plot for tensile stress with respect to Z-X orientation.

Parts made with 100% highly aged powder, without post-heating, show multiple layers of insufficiently melted particles. However, post-heating of the powder results in a denser surface with fewer non-molten particles and reduced porosity, iii) For parts made with a 50/50 mix of new and aged powder, and appropriate post-heating, the non-molten particles disappear, resulting in smooth, flat surfaces with minimal porosity. These surfaces are comparable to those made with 100% virgin powder, iv) When using a combination of 60% or 70% aged recycled powders and 40% or 30% virgin powders, the surface quality of the parts is significantly degraded, with irregular holes and numerous non-molten particles. However, with the appropriate post-heating, the parts become smoother with fewer non-molten particles, decreased porosity, and better densification, v) Parts made with 80% or 90% recycled powder and 10–20% virgin powder, without post-heating, exhibit multiple layers of non-molten particles and a porous structure, similar to parts made with 100% aged powder. Post-heating (e.g., 330 seconds) results in smooth, flat surfaces with almost no porosity and minimal non-molten particles, offering better surface quality than parts made with 100% virgin powder [38, 42], vi) The proportion of virgin to recycled powder primarily depends on cycle time, heating temperature, and powder exposure duration during SLS processing. These factors are crucial for maintaining the proper melt flow viscosity required for effective sintering and densification, vii) Impurities in the powder can also degrade the surface morphology and overall quality of the fabricated parts, further influencing the optimal combination of virgin and recycled powders to maintain the necessary melt flow viscosity for proper sintering and achieving dense, high-quality

5. Conclusion

The investigation into the build orientation for achieving high-quality and high-tensile strength AM parts reveals several key insights. The ultimate stress experienced by the specimens varied between 43.47 MPa and 46.15 MPa, indicating a notable range in mechanical properties depending on orientation. To enable manufacturers to produce parts in any orientation while minimizing anisotropy, it is crucial to maintain the mechanical integrity of the final product. Among the orientations tested, parts built in the z-axis exhibited the lowest tensile strength, while those produced in the x-axis orientation displayed the highest values. These findings support the recommendation that, for optimal tensile strength, parts should be oriented with their largest dimensions in the X-Y plane, minimizing the height (z-axis) of the part during manufacturing. According to S/N raio, part should be oriented along 0 0 90 orientation.

Additionally, the study highlights the significant role of powder material properties in achieving superior surface quality. The combination of new and aged PA2200 powders in the SLS process, coupled with post-heating treatment, demonstrated improved surface characteristics, especially when reusing reclaimed powders. This combination proves to be a promising strategy for enhancing the overall quality of parts and ensuring more consistent results in the SLS process. Furthermore, exploring different powder mixtures offers valuable potential for improving surface quality, ultimately contributing to the sustainability and cost-effectiveness of producing high-quality AM parts with reclaimed materials. This research lays the groundwork for further developments in powder reuse strategies, paving the way for more reliable and efficient additive manufacturing prac-

tices in the SLS industry.

References

[1] Tiwari SK, Pande S, Agrawal S, Bobade SM. Selection of selective laser sintering materials for different applications. Rapid Prototyping Journal. 2015;21:630–648.

[2] Gorana F, Modi YK. Influence of build orientation on porosity, strength and dimensional accuracy of laser sintered polyamide porous bone scaffolds. Archive of Mechanical Engineering. 2024;71:227–249.

[3] Vasquez M. Analysis and development of new materials for polymer laser sintering [dissertation]. Loughborough (UK): Loughborough University; 2012.

[4] Dotchev K, Yusoff W. Recycling of polyamide 12 based powders in the laser sintering process. Rapid Prototyping Journal. 2009;15:192–203.

[5] Yu G, Ma J, Li J, Wu J, Yu J, Wang X. Mechanical and tribological properties of 3D printed polyamide 12 and SiC/PA12 composite by selective laser sintering. Polymers. 2022;14:2167.

[6] Ngo TD, Kashani A, Imbalzano G, Nguyen KT, Hui D. Additive manufacturing (3D printing): A review of materials, methods, applications and challenges. Composites Part B: Engineering. 2018;143:172–196.

[7] Salmoria GV, Paggi RA, Lago A, Beal VE. Microstructural and mechanical characterization of PA12/MWCNTs nanocomposite manufactured by selective laser sintering. Polymer Testing. 2011;30:611–615.

[8] Brighenti R, Cosma MP, Marsavina L, Spagnoli A, Terzano M. Laser-based additively manufactured polymers: A review on processes and mechanical models. Journal of Materials Science. 2021;56:961–998.

[9] Ligon SC, Liska R, Stampfl J, Gurr M, Mülhaupt R. Polymers for 3D printing and customized additive manufacturing. Chemical Reviews. 2017;117:10212–10290.

[10] Kruth JP, Badrossamay M, Yasa E, Deckers J, Thijs L, Van Humbeeck J. Part and material properties in selective laser melting of metals. In: Proceedings of the 16th International Symposium on Electromachining; 2010. p. 3–14.

[11] Goodridge RD, Tuck CJ, Hague RJM. Laser sintering of polyamides and other polymers. Progress in Materials Science. 2012;57:229–267.

[12] Alimardani M. Multi-physics analysis of laser solid freeform fabrication [dissertation]. Waterloo (CA): University of Waterloo; 2009.

[13] EOS GmbH. A standard operating manual for Formiga P100. Munich (DE): EOS GmbH; 2011.

[14] Gibson I, Shi D. Material properties and fabrication parameters in selective laser sintering process. Rapid Prototyping Journal. 1997;3:129–136.

[15] Caulfield B, McHugh PE, Lohfeld S. Dependence of mechanical properties of polyamide components on build parameters in the SLS process. Journal of Materials Processing Technology. 2007;182:477–488.

[16] Rodríguez AG, Mora EE, Velasco MA, Tovar CAN. Mechanical properties of polyamide 12 manufactured by means of SLS: Influence of wall thickness and build direction. Materials Research Express. 2023;10:105304.

[17] Sanders B, Cant E, Jenkins M. Re-use of polyamide-12 in powder bed fusion and its effect on process-relevant powder characteristics and final part properties. Additive Manufacturing. 2024;80:103961.

[18] Tomanik M, Żmudzińska M, Wojtków M. Mechanical and structural evaluation of the PA12 desktop selective laser sintering printed parts regarding printing strategy. 3D Printing and Additive Manufacturing. 2021;8:271–279.

[19] Kruth JP, Levy G, Klocke F, Childs TH. Consolidation phenomena in laser and powder-bed based layered manufacturing. CIRP Annals. 2007;56:730–759.

[20] Simchi A. Direct laser sintering of metal powders: Mechanism, kinetics and microstructural features. Materials Science and Engineering A. 2006;428:148–158.

[21] Shi Y, Li Z, Sun H, Huang S, Zeng F. Effect of the properties of the polymer materials on the quality of selective laser sintering parts. Proceedings of the Institution of Mechanical Engineers Part L: Journal of Materials Design and Applications. 2004;218:247–252.

[22] Razaviye MK, Tafti RA, Khajehmohammadi M. An investigation on mechanical properties of PA12 parts produced by a SLS 3D printer: An experimental approach. CIRP Journal of Manufacturing Science and Technology. 2022;38:760–768.

[23] Eichenhofer M, Maldonado JI, Klunker F, Ermanni P. Analysis of processing conditions for a novel 3D-composite production technique. In: 20th International Conference on Composite Materials; 2015. p. 1–12.

[24] Schmid M, Wegener K. Thermal and molecular properties of polymer powders for selective laser sintering (SLS). AIP Conference Proceedings. 2016;1779:1.

[25] Gibson I. Additive manufacturing technologies: rapid prototyping to direct digital manufacturing. 1st ed. United Kingdom: Springer; 2010.

[26] Yang F, Zobeiry N, Mamidala R, Chen X. A review of aging, degradation, and reusability of PA12 powders in selective laser sintering additive manufacturing. Materials Today Communications. 2023;34:105279.

[27] Bassoli E, Gatto A, Iuliano L. Joining mechanisms and mechanical properties of PA composites obtained by selective laser sintering. Rapid Prototyping Journal. 2012;18:100–108.

[28] Zárybnická L, Petrů J, Krpec P, Pagáč M. Effect of additives and print orientation on the properties of laser sintering-printed polyamide 12 components. Polymers. 2022;14:1172.

[29] Pilipović A, Ilinčić P, Tujmer M, Rujnić Havstad M. Impact of part positioning along chamber Z-axis and processing parameters in selective laser sintering on polyamide properties. Applied Sciences. 2024;14:976.

[30] Jevtić I, Mladenović G, Milovanović A, Trajković I, Đurković M, Korolija N, Milošević M. The influence of printing orientation on the flexural strength of PA 12 specimens produced by SLS. Science of Sintering. 2024;56:45–57.

[31] Krönert M, Schuster TJ, Zimmer F, Holtmannspötter J. Creep behavior of polyamide 12, produced by selective laser sintering with different build orientations. The International Journal of Advanced Manufacturing Technology. 2022;121:3285–3294.

[32] Bai J, Yuan S, Chow W, Chua CK, Zhou K, Wei J. Effect of surface orientation on the tribological properties of laser sintered polyamide 12. Polymer Testing. 2015;48:111–114.

[33] El Magri A, Bencaid SE, Vanaei HR, Vaudreuil S. Effects of laser power and hatch orientation on final properties of PA12 parts produced by selective laser sintering. Polymers. 2022;14:3674.

[34] Calignano F, Giuffrida F, Galati M. Effect of the build orientation on the mechanical performance of polymeric parts produced by multi jet fusion and selective laser sintering. Journal of Manufacturing Processes. 2021;65:271–282.

[35] Baba MN. Flatwise to upright build orientations under three-point bending test of Nylon 12 (PA12) additively manufactured by SLS. Polymers. 2022;14:1026.

[36] Slager JJ, Earp BC, Ibrahim AM. Influence of build orientation and part thickness on tensile properties of polyamide 12 parts manufactured by selective laser sintering. Polymers. 2024;16:2241.

[37] Nelson JA, Galloway G, Rennie AE, Abram TN, Bennett GR. Effects of scan direction and orientation on mechanical properties of laser sintered polyamide-12. International Journal of Advanced Design and Manufacturing Technology. 2014;7.

[38] Yang F, Jiang T, Lalier G, Bartolone J, Chen X. Process control of surface quality and part microstructure in selective laser sintering involving highly degraded polyamide 12 materials. Polymer Testing. 2021;93:106920.

[39] Guo B, Xu Z, Luo X, Bai J. A detailed evaluation of surface, thermal, and flammable properties of polyamide 12/glass beads composites fabricated by multi jet fusion. Virtual and Physical Prototyping. 2021;16:S39–S52.

[40] Balan GS, Raj SA, Adithya RN. Effect of post-heat treatment on the mechanical and surface properties of nylon 12 produced via material extrusion and selective laser sintering processes. Polymer Bulletin. 2024.

[41] Kumar S. Selective laser sintering: A qualitative and objective approach. JOM. 2003;55:43–47.

[42] Higa CF. Selective laser sintering of Copper-Nickel and Molybdenum alloys to be used as EDM electrodes [master's thesis]. Parana (BR): Pontifical Catholic University of Parana; 2011.

[43] Yang F, Chen X. A combined theoretical and experimental approach to model polyamide 12 degradation in selective laser sintering additive manufacturing. Journal of Manufacturing Processes. 2021;70:271–289.

[44] Han W, Kong L, Xu M. Advances in selective laser sintering of polymers. International Journal of Extreme Manufacturing. 2022;4:042002.

[45] O'Connor HJ, Dowling DP. Comparison between the properties of polyamide 12 and glass bead filled polyamide 12 using the multi jet fusion printing process. Additive Manufacturing. 2020;31:100961.

[46] Tofail SA, Koumoulos EP, Bandyopadhyay A, Bose S, O'Donoghue L, Charitidis C. Additive manufacturing: scientific and technological challenges, market uptake and opportunities. Materials Today. 2018;21:22–37.

[47] Mehdipour F, Gebhardt U, Kästner M. Anisotropic and rate-dependent mechanical properties of 3D printed polyamide 12–A comparison between selective laser sintering and multi jet fusion. Results in Materials. 2021;11:100213.

[48] Gomes PC, Piñeiro OG, Alves AC, Carneiro OS. On the reuse of SLS polyamide 12 powder. Materials. 2022;15:5486.

[49] Haleem A, Javaid M, Khan S, Khan MI. Retrospective investigation of flexibility and their factors in additive manufacturing systems. International Journal of Industrial and Systems Engineering. 2020;36:400–429.

[50] ASTM International. Standard test method for tensile properties of plastics. ASTM D638-10; 2010.

[51] ASTM International. Standard terminology for additive manufacturing – coordinate systems and test methodologies. ASTM 52921; 2013.